Laboratory Investigation

Degradable PLGA Scaffolds with Basic Fibroblast Growth Factor

Experimental Studies in Myocardial Revascularization

Ying Wang, PhD
Xiao-Cheng Liu, MD
Jian Zhao, MD
Xiang-Rong Kong, MD
Rong-Fang Shi, MD
Xiao-Bin Zhao, MD
Cun-Xian Song, PhD
Tian-Jun Liu, PhD
Feng Lu, PhD

Key words: *Angiogenesis inducing agents/administration & dosage; disease models, animal; drug delivery systems/methods; fibroblast growth factors/administration & dosage; glycolates; implants, experimental; lactic acid; myocardial infarction; myocardial ischemia; neovascularization, physiologic; polyglycolic acid; swine; tissue engineering/methods*

From: *Department of Cardiovascular Surgery (Drs. Kong, Liu X-C, Shi, Wang, Zhao J, and Zhao X), TEDA International Cardiovascular Hospital, Peking Union Medical College, Tianjin 300457; and Institute of Biomedical Engineering (Drs. Liu T-J, Lu, and Song), Peking Union Medical College, Tianjin 300192; People's Republic of China*

This work was supported by a grant from Tianjin Science & Technology Development Project (grant number 05YFGZSF02900).

Address for reprints: *Xiao-Cheng Liu, MD, Department of Cardiovascular Surgery, TEDA International Cardiovascular Hospital, No. 61, The Third Avenue, Technical Economic Development Area, Tianjin 300457, PRC*

E-mail: *zhaojian78@yahoo.com*

Our goal was to investigate the efficacy of degradable poly(D,L-lactic-coglycolic acid) (PLGA) scaffolds loaded with basic fibroblast growth factor (bFGF) in inducing cardiac neovascularization, increasing perfusion, and improving cardiac function.

For ease of scaffold implantation into the ventricular wall, we developed a channel-producing device. Mini-swine, established as the animal model, were grouped as follows: channels-alone (control) group, channels and blank scaffolds (CBS) group, and channels and bFGF-incorporating scaffolds (CFS) group. Two scaffolds were implanted in each animal in the CBS and CFS groups. Six weeks postoperatively, endothelial cells were immunohistologically stained for von Willebrand factor, and proliferating cells for Ki-67 antigen. The density of new vessels was counted by image-analysis software. Left ventricular function and myocardial perfusion were documented by echocardiography and nuclear scanning, respectively, before implantation and 6 weeks postoperatively.

The combined application of PLGA and bFGF ensured sustained release of growth factor in the target region. In the CFS group, Ki-67-positively stained cells, vascular density, and perfusion-defect percentage all showed significant improvement (P <0.001), compared with the control and CBS groups, which did not. Moreover, the left ventricular fractional shortening percentage in the CFS group (28.98% ± 1.24%) showed a significant increase, compared with the control group (26.57% ± 1.92%, P=0.009) and the CBS group (27.11% ± 0.71%, P=0.033), neither of which showed a difference (P=0.508).

The bFGF-incorporating PLGA scaffold can promote neovascular formation, enhance blood-flow perfusion, and improve myocardial function, although the original scaffold lumina were eventually occluded by inflammatory cells and scar tissue. ***(Tex Heart Inst J 2009;36(2):89-97)***

Because the number of patients who have diffuse coronary atherosclerosis not amenable to coronary artery bypass grafting or percutaneous coronary angioplasty continues to increase,[1,2] alternative therapies for improving myocardial perfusion have been explored. One promising treatment is "angiogenic biologic bypass,"[3] which is the application of exogenous angiogenic growth factors to promote collateral vascular development in ischemic regions.

Of these growth factors, basic fibroblast growth factor (bFGF) is known to be a pluripotent mitogenic polypeptide for fibroblasts, smooth muscle cells, and vascular endothelial cells, all of which are involved in neovascular formation.[4-6] In addition, bFGF is capable of inhibiting apoptosis and protecting acute ischemic myocardium[7] by regulating the expression of protein kinase C[8] and BCL-2.[9] Nonetheless, the short biological half-life of free bFGF in vivo[10] and its rapid washout from large vascular structures in myocardial interstitium[11] limit its ability to induce collateral vessel development continuously. In this setting, many studies[12-14] have explored the development of slow-release carrier systems for bFGF. However, the above-mentioned bFGF-loaded carriers were all in solution and were injected into the beating heart, which possibly led to rapid loss of drugs into the cardiac chamber when the needle penetrated the endocardium a little too deeply or when cardiac squeezing caused continuous leakage from epicardial puncture sites.[15]

On the basis of these considerations, we fabricated a novel bFGF-incorporating tubular scaffold from poly(D,L-lactic-coglycolic acid) (PLGA). The objective of this study was to investigate whether this scaffold could keep the lumen patent and, via continuous bFGF bioactivity, promote new vascular formation around the stenot-

ic artery, thereby improving myocardial perfusion and cardiac function over the level attainable through angioplasty alone.

Materials and Methods

Myocardial Infarction Model

Animals. Twenty mini-swine were secured for the experiment. All experimental animals were cared for in accordance with institutional guidelines and with the 1996 "Guide for the Care and Use of Laboratory Animals," published by the National Institutes of Health (NIH publication 85-23, revised 1996). Two of the 20 mini-swine were subsequently excluded because of intractable ventricular fibrillation after ligation.

Preparation of the Model. Eighteen mini-swine survived for the subsequent procedures. These remaining animals, each weighing 25 to 35 kg, were anesthetized intramuscularly with ketamine (10 $mg \cdot kg^{-1}$) and midazolam (0.2 $mg \cdot kg^{-1}$). After oral endotrachial intubation, anesthesia was maintained with 1% to 2% inhaled isoflurane. The 18 subjects were monitored via electrocardiography. Three million units of penicillin were given intravenously before skin incision.

Under sterile conditions, the heart was fully exposed via a median sternotomy. The middle third of the left anterior descending coronary artery (LAD) was ligated after 3 intermittent, brief preconditioning occlusions were performed in order to prevent malignant ventricular dysrhythmias. Lidocaine was given by direct intravenous injection (1 $mg \cdot kg^{-1}$) and then by intravenous drip (1 $mg \cdot min^{-1} \cdot kg^{-1}$). After the successful establishment of the model of LAD occlusion, the mini-swine were assigned to 3 groups (n=6 per group) at random: channels-alone (control) group, channels and blank scaffolds (CBS) group, and channels and bFGF-incorporating scaffolds (CFS) group.

Preparation of Scaffolds

In this study, a novel tubular biodegradable polymer scaffold (Fig. 1A) was developed. It was composed of a 50:50 mol ratio of 2 PLGA polymers (Chinese Academy of Science; Chengdu, China). The procedure was briefly performed as follows: 0.8 g PLGA and 150 µg bFGF (molecular mass, 17.4 kD; purity >97; R&D, Minneapolis, Minn) were dissolved in a 10-mL solution of dichloromethane. Then, this liquid mixture was spread into a thin, flexible film and rolled by means of a mandrel casting technique into the form of a hollow tube (outer diameter, 3.0 mm; inner diameter, 2.8 mm). The tubular PLGA was then dried (25 °C for 24 hr) in a vacuum and cut into 10 segments of 10 mm each in length. Therefore, each segment (or scaffold) had 15 µg bFGF. In the CBS group, the blank scaffolds had no bFGF. To facilitate permeation of the scaffold walls by blood, 16 regularly aligned micropores were produced within each scaffold wall by a mini power drill equipped with a 1.0-mm bit (Sandvik; Sandviken, Sweden). The scaffolds were then sterilized by means of cobalt-60 radiation and maintained at 4 °C.

Channel-Producing Procedure

Within 6 hours of the onset of infarction (that is, ligation of the LAD), we drilled transmural channels in the myocardium. Figure 1B shows the self-made hollow bit of 3.0 mm in diameter, which we used for transmural drilling. In preparation, the bit was placed perpendicularly to the epicardial surface of the beating heart; then the drill was triggered and the bit was rotated into the ventricular wall at high speed (5,000 rpm). The depth of the channel was modulated by pulling up the bit, according to the thickness of ventricular wall as measured intraoperatively by means of echocardiography. Two channels were drilled in the infarcted area of each heart. Transmural penetration was confirmed by loss of resistance and pulsatile bleeding from the epicardium. The removed cylinder-shaped plug of tissue, under the pressure of cardiac contraction, was instantaneously flushed

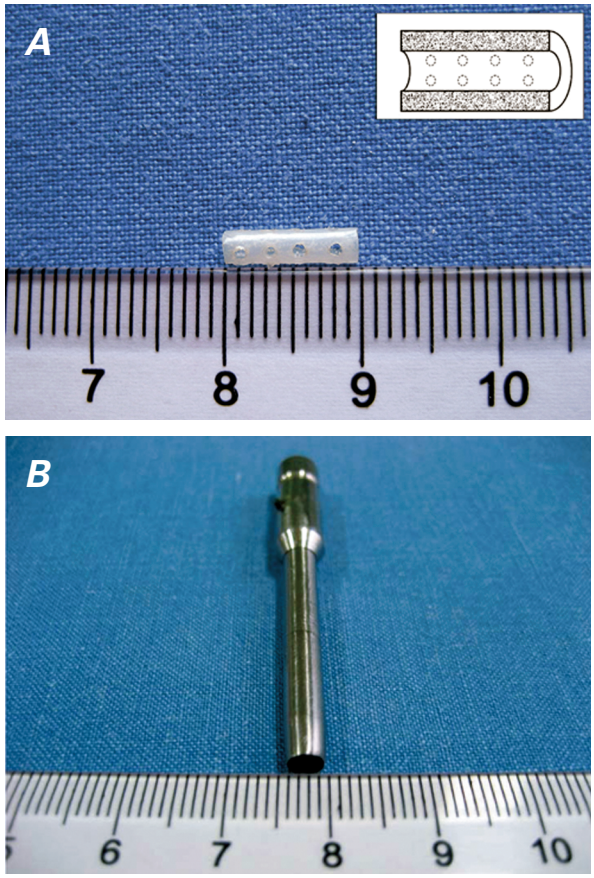

Fig. 1 ***A****) The poly(D,L-lactic-coglycolic acid) (PLGA) scaffold is 10 mm in length, with 16 regularly aligned micropores. Inset: the scaffold in profile.* ***B****) The hollow bit for drilling transmural channels has an internal diameter of 3 mm.*

from the hole at the upper end of the bit. The scaffold was immediately implanted into the channel. Bleeding was controlled by means of shallow epicardial purse-string stitches that had been placed in advance, which also served as markers of the channel sites 6 weeks later. In the control group, the entire procedure, including the purse-string stitches but excluding the scaffold placement, was performed. The pericardium was left widely open, the chest was closed in layers in routine fashion, and anesthesia was reversed. Antibiotics were administered intramuscularly for 3 days postoperatively.

Echocardiographic Evaluation

In all groups, echocardiography was performed intraoperatively before implantation and again 6 weeks postoperatively. The echocardiographer was blinded to the experimental groups, and echocardiograms were obtained with an echocardiography system (Philips® SONOS 7500 Ultrasound, Royal Philips Electronics; Best, The Netherlands) equipped with a 1.6- to 3.2-MHz transducer. The images were obtained by placing the transducer almost directly on the epicardial surface to avoid the influence of the protuberant sternum and thick adipose layer. Between the epicardium and the transducer we placed a water sac of our own manufacture in order to avoid the loss of ultrasonic waves in the near field.

M-Mode images were obtained through the long axis of the channel at the anteroapical level and were calculated further for the following measurements in millimeters: left ventricular end-diastolic dimension (LVEDd) and left ventricular end-systolic dimension (LVEDs). Left ventricular fractional shortening (FS%) was inferred as (LVEDd – LVEDs)/LVEDd × 100.

Myocardial Perfusion Evaluation

Myocardial perfusion was evaluated by intravenously injecting ^{99m}Tc-sestamibi (14.8 MBq·kg^{-1}) before implantation and again 6 weeks postoperatively. Myocardial perfusion images were acquired at 6° per frame, totally for 180° by rotating a 64×64 matrix detector in a 20% energy window using echocardiographic-gated single-photon-emission computed tomography (SPECT) Millennium VG-5, GE Healthcare; Chalfont St. Giles, UK), with reconstruction parameters as follows: pre-filter, Butterworth; critical frequency, 0.52; and power, 5.0. Quantitative analysis of changes of MDP (mass defection of percentage) was performed by Emory Cardiac Toolbox™ software (ECTb, Syntermed, Inc.; Atlanta, Ga). Mass defection of percentage was used as an index of perfusion defect: MDP = (Md/Mt) ×100. The mass of ischemic-related myocardial defect (Md) and that of total myocardium (Mt) were calculated by tomographic reconstruction. Changes in MDP were calculated as MDP 6 weeks postoperatively minus baseline MDP before implantation.

Histologic Staining

Six weeks postoperatively, the animals were killed with an overdose of potassium chloride, and their hearts were harvested for histologic analysis. The locations of the channels were readily identified by the sutures on the epicardial surface. Heart samples were immediately immersed into 4% formaldehyde in phosphate-buffered saline of pH 7.4 at 4 °C for 24 hours. After fixation, the samples were embedded in paraffin and sectioned in 5-µm-thick slices. Routine staining was performed with hematoxylin-eosin. Vascular endothelial cells were identified by von Willebrand factor immunohistochemical staining, which was performed as follows: the sections were incubated with 1:100 von Willebrand factor antibody (Dako Denmark A/S; Glostrup, Denmark) in 0.1% phosphate-buffered saline for 1 hour, then counter-stained with diaminobenzidene. Fifty non-overlapping fields per group were randomly captured with a video camera at ×100 magnification in transverse sections and then digitized into tagged-image file format (TIFF). New vessels were quantified with use of the Image-Pro Plus 4.5 software package (Media Cybernetics, Inc.; Bethesda, Md). The positively stained areas were padded with a single color and converted to pixels through optical density calibration (Figs. 2A–C).

In addition, tissue sections were stained with Ki-67 antibody (Dako) to reveal the number of proliferating cells. Fifty non-overlapping fields per group were randomly captured at ×400 magnification in transverse sections.

Statistical Analysis

Results are presented as mean ± SD. One-way analysis of variance (ANOVA) was used to evaluate differences among all groups in vascular density, proliferating cells, changes in MDP, and FS%. Least-significant-difference tests were used to detect between-group differences. All statistical tests were 2-tailed, and $P<0.05$ was regarded as statistically significant.

Results

Death and Injury Assessment

Aside from the 2 mini-swine that were excluded from the experiment because of intractable ventricular fibrillation after ligation, there were no subsequent problems with injury and no deaths. Scaffold implantation did not induce severe events involving malignant arrhythmias, embolization, bleeding, hemodynamic abnormality, and the like.

Histologic Analysis

In the CFS group, the hematoxylin-eosin images displayed a large number of new vessels and surrounding (albeit scattered) inflammatory cells. There also occurred some small vesiculous polymer remnants, which

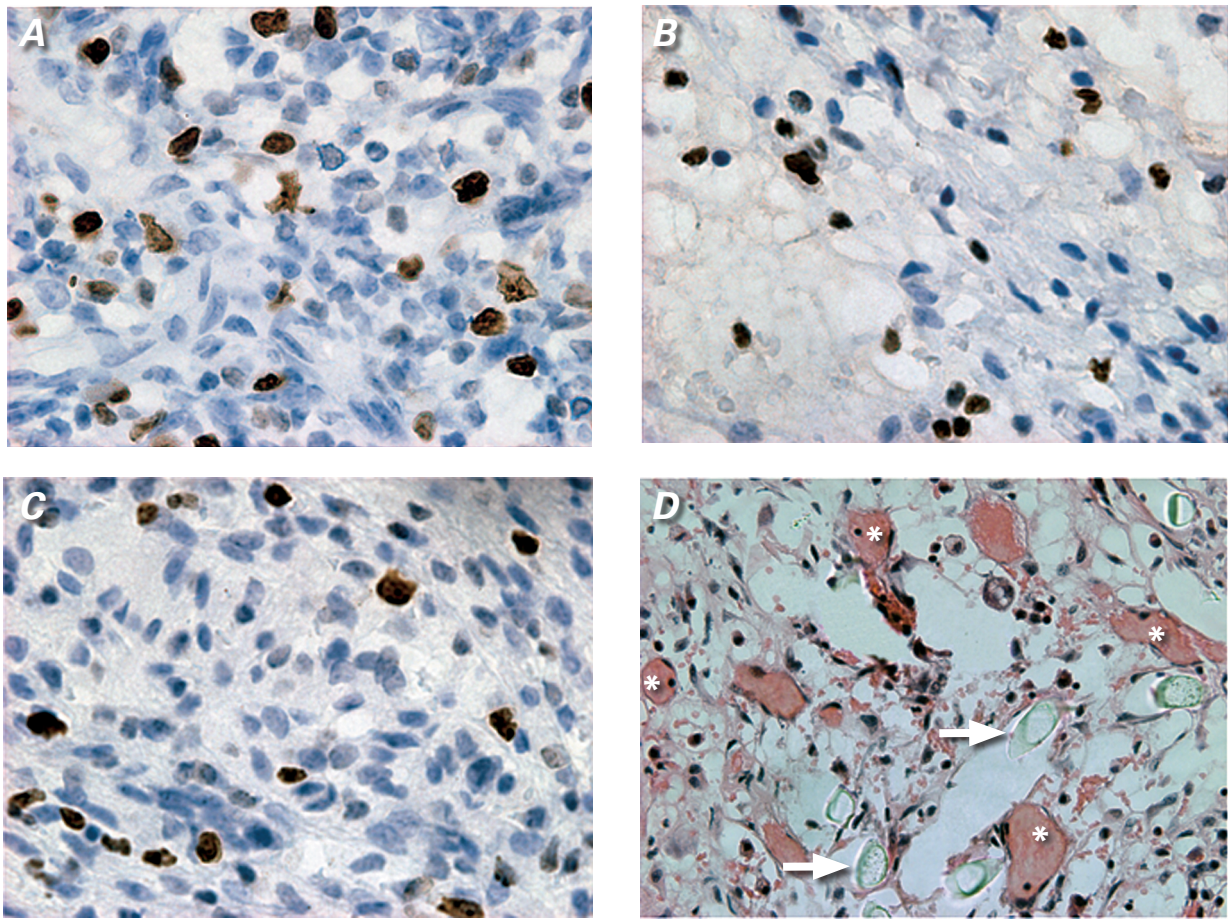

Fig. 2 *Representative images obtained by Ki-67 immunohistologic and hematoxylin-eosin staining: Ki-67 positively stained S-stage cells in CFS group (**A**), in channels and blank scaffolds (CBS) group (**B**), and in control group (**C**) (3'3-diaminobenzidine HCl, orig. ×400). New vessels within the bFGF-incorporating scaffold (CFS) group (**D**) (* indicates new vessels, arrows indicate polymer remnants; H & E, orig. ×200).*

appeared to act as pro-angiogenic cores and to provide a suitable platform for the attachment of endothelial cells and for vascular remodeling. Perivascular spindle-like endothelial cells formed round or oval lumina with the passage of red-stained blood components (Fig. 2D), although the original lumina of the scaffolds were almost completely obliterated. In Ki-67 immunohistologic staining, the number of proliferating cells per high-power field (hpf) in the CFS group (21.3 ± 3.6 cells/hpf) markedly increased compared with the numbers in the CBS group (13.7 ± 3.6 cells/hpf, P=0.002) and in the control group (12.4 ± 4.8 cells/hpf, P <0.001). Image-Pro Plus software analysis (Fig. 3) revealed that vascular density in the CFS group (5,934 ± 313 pixels/hpf, P <0.001 for all differences) increased significantly in comparison with vascular density in the CBS group (2,655 ± 373 pixels/hpf) and in the control group (2,581 ± 428 pixels/hpf).

SPECT Evaluation

Figure 4 illustrates SPECT measurements for all groups. The SPECT images showed perfusion improvements (Fig. 4A) in the CFS group at 6 postoperative weeks, compared with perfusion before therapy. The ECTb software (Fig. 4B) showed significant perfusion-defect decreases in the CFS group (–1.12% ± 0.28%, P <0.001 for all differences), compared with the CBS group (–2.12% ± 0.13%) and the control group (–2.06% ± 0.20%), neither of which showed any difference in between-group comparison (P=0.642).

Echocardiographic Evaluation

Echocardiographic images (Fig. 5A) from the left ventricular short axis clearly showed the scaffold's long-axis profile, the lumen of which was expressed as weak resonance. Baseline FS% before implantation (Fig. 5B) did not show any difference between any of the 3 groups (P=0.834). However, 6 weeks postoperatively, significant increases of FS% were shown in the CFS group (28.98% ± 1.24%), in comparison with both the CBS group (27.11% ± 0.71%, P=0.033) and the control group (26.57% ± 1.92%, P=0.009), neither of which showed any difference in between-group comparison (P=0.508).

Discussion

Basic fibroblast growth factor is widely known as a pluripotent mitogenic polypeptide for fibroblasts, smooth muscle cells, and vascular endothelial cells, all of which are involved in neovascular formation.[4-6] However, the short biological half-life of free bFGF has been resolved by using degradable polymeric materials as carriers for local delivery of the bioactive agent. These include hydrogel,[13,16,17] chitosan hydrogel,[18] alginate,[12] collagen,[14] and PLGA.[7,19] Of these, PLGA, due to its superior biodegradability and biocompatibility in vivo, has been approved by the U.S. Food and Drug Administration and is widely used as a controlled-release carrier of various exogenous agents.[20-22] In our study, the PLGA scaffold, as expected, did not lead to systemic side effects such as embolism, bleeding, and hemodynamic abnormality. Moreover, the PLGA scaffold can be programmed to degrade over a predictable period of time that will coincide with the period of new vascular formation,[23] by adjusting the proportion of polylactic to glycolic acid. Finally, a bFGF-incorporating scaffold can more efficiently transport drugs to the ischemic target sites, in comparison with other routes of administration (intravenous,[24] intracoronary,[25] retrograde coronary venous,[26,27] and intrapericardial[28,29]).

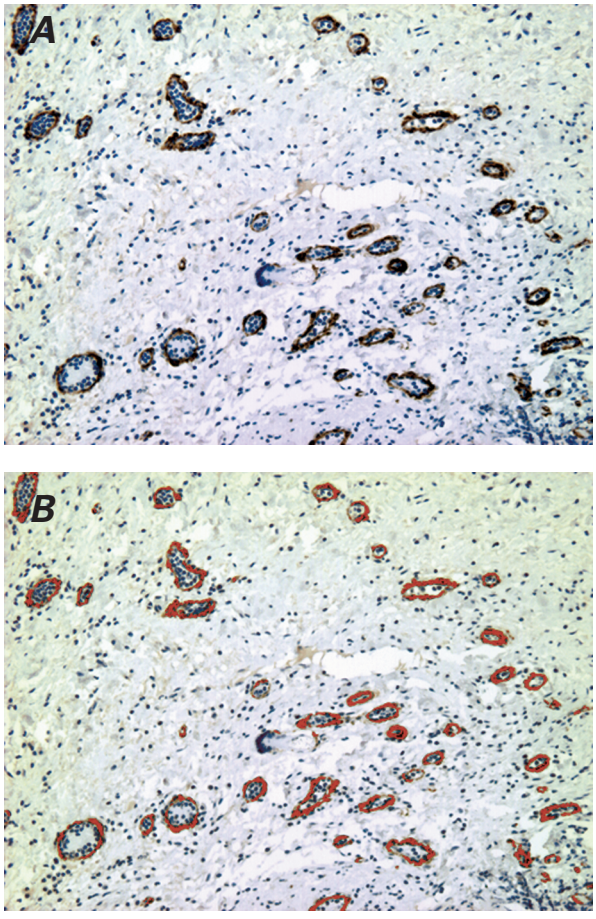

Fig. 3 *Here we see von Willebrand factor immunohistologic staining, followed by Image-Pro Plus analysis:* ***A****) von Willebrand factor positively stained vessels in the bFGF-incorporating scaffold group (DAB, orig. ×100);* ***B****) the same von Willebrand factor–stained vascular walls, padded precisely with a single red color by Image-Pro Plus software.*

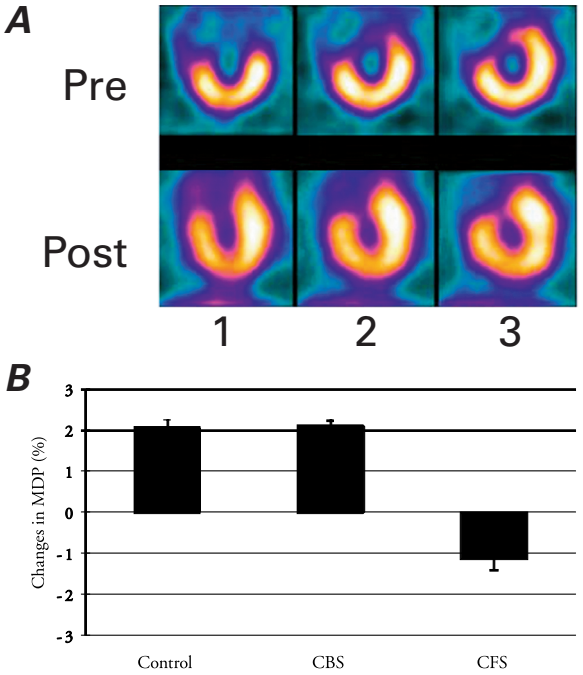

Fig. 4 ***A****) Representative single-photon-emission computed tomographic images in the bFGF-incorporating scaffold group.* ***B****) Changes in MDP (mass defection of percentage) in all groups, as indicated by Emory Cardiac Toolbox™ software analysis.*

1 = vertical short axis; 2 = horizontal long axis; 3 = vertical long axis; CBS = channels and blank-scaffold group; CFS = channels and bFGF-incorporating scaffold group; Pre = preimplantation; Post = 6 weeks postoperatively

Administration via the intrapericardial route has been said to lead to "a transmural gradient of bFGF from epimyocardium to endomyocardium, with approximately an order of magnitude difference between the two." This has been reported in the findings of Uchida[30] and Laham[28] and their respective groups. Much more of the drug (19%) has been shown to be present (localized to the heart) 150 minutes after administration via the intrapericardial route than via the intracoronary or left atrial route.[31] The transmural gradient might be caused by epicardial connective tissue as an obstacle to drug penetration to the myocardium. The existence of such an obstacle, however, runs contrary to the true clinical features displayed by patients during episodes of angina pectoris, when the endomyocardium often suffers more severe myocardial ischemia than does the epimyocardium.

Similarly, direct intramyocardial injection, although not impeded by the epicardium, resulted in poor drug

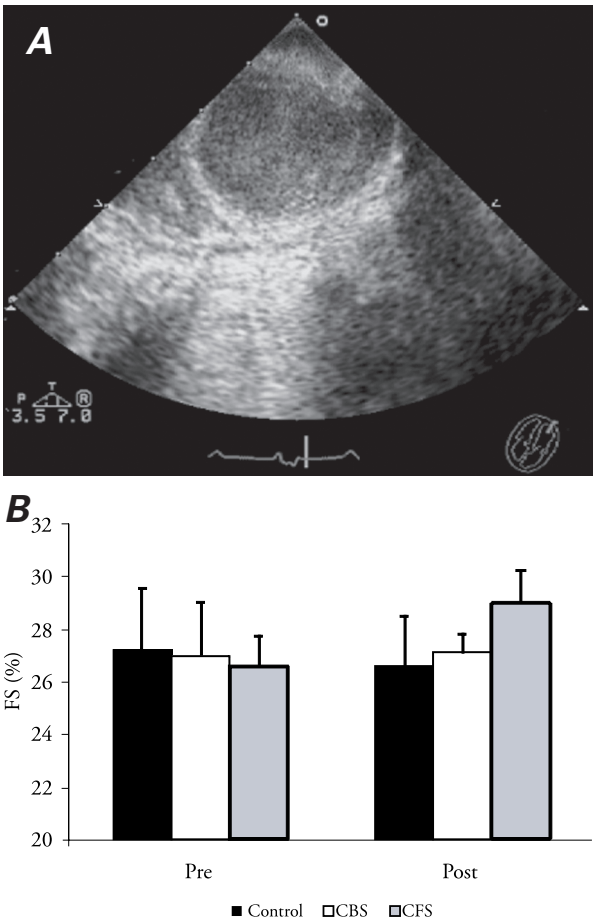

Fig. 5 ***A****) Representative echocardiographic image of scaffold in the anteroapical region.* ***B****) Left ventricular fractional shortening percentage (FS%) of all groups before implantation and 6 weeks postoperatively.*

CBS = channels and blank-scaffold group; CFS = channels and bFGF-incorporating scaffold group; Pre = preimplantation; Post = 6 weeks postoperatively

distribution. In practice, there has always been difficulty in precise regulation of the needle depth when injecting the beating heart. Imprecise injection, whether too deep or too shallow, might not distribute drugs throughout the full thickness of the ventricular wall. Teng and associates[15] demonstrated another limitation of intramyocardial administration in a beating heart: 88.9% of injected microspheres were squeezed out by contractions of the myocardium, resulting in a great disparity between administered dosage and retained dosage. We encountered this same problem in our earlier experiments.[32] For this new experiment, we developed a tubular scaffold that we could easily implant into a channel of compatible diameter for the uniform distribution of drugs along the full thickness of the ventricular wall, little influenced by the contractile movement of the heart.

With the aid of the PLGA scaffold as a carrier, bFGF, when released slowly from polymeric materials, can maintain its bioactivity and act continuously in both mitogenic and chemoattractant roles to induce various S-stage cellular proliferations and extracellular matrix ingrowth. Previous studies have shown that both recruited and proliferating cells—whether monocytes and macrophages[33-35] or endothelial cells and fibroblasts[36]—are involved in vascular reconstruction,[37-39] and we found this same result in sites where scaffolds had been implanted. Immunohistologic staining with Ki-67 and hematoxylin-eosin (Fig. 2D) both showed a large number of new vessels in areas where there were influxes of proliferating cells (that is, areas where red-stained blood components had passed). The vesiculous polymer remnants also served as a scaffold in milieu, providing a suitable platform for the sprouting of endothelial cells, migration, and attachment. In addition, the Ki-67-positive cells also could have released a number of pro-angiogenic factors, including vascular endothelial growth factor (VEGF), transforming growth factor β3 (TGF-β3), interleukin 1-β (IL-1β), and von Willebrand factor,[40,41] which synergistically promoted neovascularization. Consequential to blood-flow increases were significant improvements in cardiac function, largely attributable to the recovery of hypodynamic "hibernating" myocardium.

In those previous studies, there existed great differences in the bFGF dose that was administered, ranging from 225 ng per mongrel dog[42] to 200 μg per rat.[43] In mini-swine with an average weight of 25 to 35 kg, Biswas and associates[44] administered bFGF dosages of 0.6 μg/kg and 6 μg/kg, corresponding to total doses per animal of 15 to 21 μg and 150 to 210 μg. They reported that bFGF doses of 150 to 210 μg did not result in significant increases in myocardial blood flow, compared with the much lower doses of 15 to 21 μg. This result was consistent with coronary resistance data from Lopez and associates,[45] who suggested the existence of a plateau effect between 20 to 30 μg of bFGF. Further, Baffour and colleagues revealed that high doses of bFGF inhibit angiogenesis and collateral circulation, in comparison with moderate doses.[46] In our study, the bFGF dose carried by each scaffold was 15 μg. In order to increase blood perfusion through the scaffold wall, we drilled 16 regular micropores within each wall, which inevitably led to drug loss. The loss percentage was calculated after spreading the tubular scaffold to its original rectangular shape. Because the thickness of the scaffold was the same whether in tubular or rectangular form, the loss percentage was expressed as a ratio of the area of 16 round micropores to the rectangle, as represented in 2-dimensional profile (Fig. 6). The effective dosage of each scaffold was then 13 μg in vivo. Consequently, each animal received a total of 26 μg bFGF from 2 scaffolds.

In this study, the control group received transmural channels (instead of myocardial infarction alone) as did

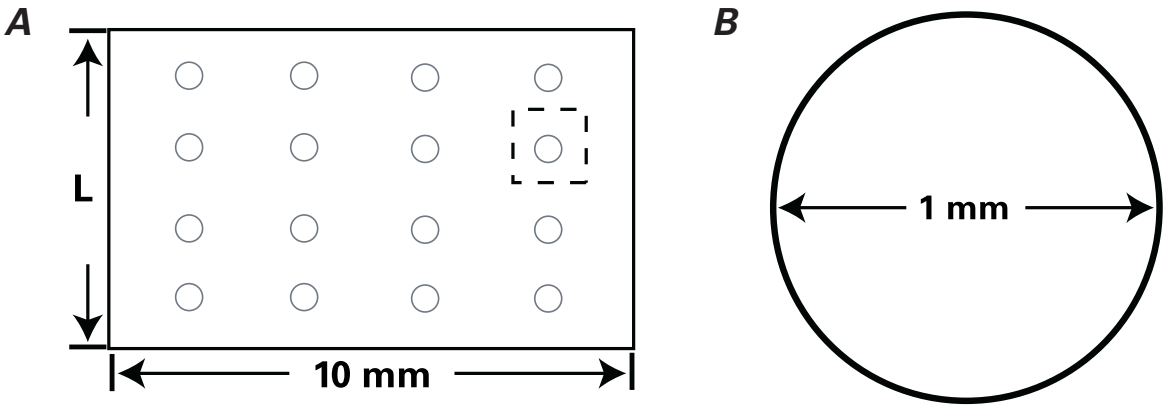

Fig. 6 ***A****) Diagram of a scaffold spread into a rectangle. Area (S1): 10·L=10·3π=30π mm², (L=π·D=3π mm²).* ***B****) Diagram of a single micropore in cross-section. The area of 16 microspheres (S2): 16π·r² =16·π·(0.5)2=4π mm². Loss percentage: S1/S2=4/30≈13%. Lost dosage: 15 μg·4/30=2 μg.*

the other 2 groups, in order to reduce errors in counting vessels and in making between-group comparisons: the channels alone could induce angiogenesis by nonspecific inflammatory response.[47] Similarly, all the groups underwent epicardial purse-string suturing; even acupuncture, to some extent, could promote new vessel formation.[48]

The PLGA polymer was formed into a hollow tubular scaffold by mandrel casting in order to mimic myocardial sinusoids and transmyocardial laser channels in our investigation of ways to convey blood directly to ischemic tissue. The channels themselves were obliterated by fibrosis 6 weeks postoperatively. The PLGA scaffold, as a foreign body, possibly caused adhesion and aggregation of platelets. On the other hand, tissue injury from drilling the transmural channels would have triggered a coagulation cascade instantly by activating factors III and XII. In a future study, we will incorporate heparin into the slow-release PLGA polymer, thereby attempting to maintain patency by continuously inhibiting the coagulation pathway.

Limitations

We realize that the present study has these limitations: 1) We chose an acute myocardial infarction model as our experimental setting, in order to reperfuse the "dying" ischemic myocardium in much the same way as emergent percutaneous coronary angioplasty and scaffolding does, within the first 6 hours of infarction onset. But in an actual hospital setting, more patients are admitted and treated for chronic myocardial ischemia, characterized by infarcted and even fibrous myocardium. Therefore, the use of experimental subjects with chronic ischemia might have been more practical. 2) The optimal density of scaffold implantation in patients who have diverse areas of infarction remains unclear. 3) The optimal bFGF dose for administration via this scaffold approach needs to be clarified, as does the synergism of this controlled-release therapy in combination with that of other growth factors,[49] such as VEGF, TGF, and angiopoietin-1.

Conclusions

A PLGA scaffold that incorporates bFGF was able to induce neovascular formation, enhance blood-flow perfusion, and improve cardiac function, although the original scaffold channels that mimicked myocardial sinusoids were eventually occluded.

References

1. Mukherjee D, Bhatt DL, Roe MT, Patel V, Ellis SG. Direct myocardial revascularization and angiogenesis--how many patients might be eligible? Am J Cardiol 1999;84(5):598-600, A8.
2. Henry TD. Therapeutic angiogenesis. BMJ 1999;318(7197):1536-9.
3. Syed IS, Sanborn TA, Rosengart TK. Therapeutic angiogenesis: a biologic bypass. Cardiology 2004;101(1-3):131-43.
4. Poole TJ, Finkelstein EB, Cox CM. The role of FGF and VEGF in angioblast induction and migration during vascular development. Dev Dyn 2001;220(1):1-17.
5. Cox CM, Poole TJ. Angioblast differentiation is influenced by the local environment: FGF-2 induces angioblasts and patterns vessel formation in the quail embryo. Dev Dyn 2000;218(2):371-82.
6. Parsons-Wingerter P, Elliott KE, Clark JI, Farr AG. Fibroblast growth factor-2 selectively stimulates angiogenesis of small vessels in arterial tree. Arterioscler Thromb Vasc Biol 2000;20(5):1250-6.
7. Kardami E, Detillieux K, Ma X, Jiang Z, Santiago JJ, Jimenez SK, Cattini PA. Fibroblast growth factor-2 and cardioprotection. Heart Fail Rev 2007;12(3-4):267-77.
8. Jiang ZS, Padua RR, Ju H, Doble BW, Jin Y, Hao J, et al. Acute protection of ischemic heart by FGF-2: involvement of FGF-2 receptors and protein kinase C. Am J Physiol Heart Circ Physiol 2002;282(3):H1071-80.
9. Karsan A, Yee E, Poirier GG, Zhou P, Craig R, Harlan JM. Fibroblast growth factor-2 inhibits endothelial cell apopto-

sis by Bcl-2-dependent and independent mechanisms. Am J Pathol 1997;151(6):1775-84.
10. Whalen GF, Shing Y, Folkman J. The fate of intravenously administered bFGF and the effect of heparin. Growth Factors 1989;1(2):157-64.
11. Laham RJ, Post M, Rezaee M, Donnell-Fink L, Wykrzykowska JJ, Lee SU, et al. Transendocardial and transepicardial intramyocardial fibroblast growth factor-2 administration: myocardial and tissue distribution. Drug Metab Dispos 2005; 33(8):1101-7.
12. Sellke FW, Laham RJ, Edelman ER, Pearlman JD, Simons M. Therapeutic angiogenesis with basic fibroblast growth factor: technique and early results. Ann Thorac Surg 1998;65(6): 1540-4.
13. Yamamoto M, Ikada Y, Tabata Y. Controlled release of growth factors based on biodegradation of gelatin hydrogel. J Biomater Sci Polym Ed 2001;12(1):77-88.
14. Nillesen ST, Geutjes PJ, Wismans R, Schalkwijk J, Daamen WF, van Kuppevelt TH. Increased angiogenesis and blood vessel maturation in acellular collagen-heparin scaffolds containing both FGF2 and VEGF. Biomaterials 2007;28 (6):1123-31.
15. Teng CJ, Luo J, Chiu RC, Shum-Tim D. Massive mechanical loss of microspheres with direct intramyocardial injection in the beating heart: implications for cellular cardiomyoplasty. J Thorac Cardiovasc Surg 2006;132(3):628-32.
16. Thompson JA, Anderson KD, DiPietro JM, Zwiebel JA, Zametta M, Anderson WF, Maciag T. Site-directed neovessel formation in vivo. Science 1988;241(4871):1349-52.
17. Miyoshi M, Kawazoe T, Igawa HH, Tabata Y, Ikada Y, Suzuki S. Effects of bFGF incorporated into a gelatin sheet on wound healing. J Biomater Sci Polym Ed 2005;16(7):893-907.
18. Fujita M, Ishihara M, Morimoto Y, Simizu M, Saito Y, Yura H, et al. Efficacy of photocrosslinkable chitosan hydrogel containing fibroblast growth factor-2 in a rabbit model of chronic myocardial infarction. J Surg Res 2005;126(1):27-33.
19. Ruel M, Laham RJ, Parker JA, Post MJ, Ware JA, Simons M, Sellke FW. Long-term effects of surgical angiogenic therapy with fibroblast growth factor 2 protein. J Thorac Cardiovasc Surg 2002;124(1):28-34.
20. Elcin AE, Elcin YM. Localized angiogenesis induced by human vascular endothelial growth factor-activated PLGA sponge. Tissue Eng 2006;12(4):959-68.
21. Schindler A, Jeffcoat R, Kimmel G, Pitt C, Wall M, Zweidinger R. Biodegradable polymers for sustained drug delivery. Contemp Top Polym Sci 1977;2:251-87.
22. Wei G, Jin Q, Giannobile WV, Ma PX. Nano-fibrous scaffold for controlled delivery of recombinant human PDGF-BB. J Control Release 2006;112(1):103-10.
23. Grayson AC, Voskerician G, Lynn A, Anderson JM, Cima MJ, Langer R. Differential degradation rates in vivo and in vitro of biocompatible poly(lactic acid) and poly(glycolic acid) homo- and co-polymers for a polymeric drug-delivery microchip. J Biomater Sci Polym Ed 2004;15(10):1281-304.
24. Edelman ER, Nugent MA, Karnovsky MJ. Perivascular and intravenous administration of basic fibroblast growth factor: vascular and solid organ deposition. Proc Natl Acad Sci U S A 1993;90(4):1513-7.
25. Rajanayagam MA, Shou M, Thirumurti V, Lazarous DF, Quyyumi AA, Goncalves L, et al. Intracoronary basic fibroblast growth factor enhances myocardial collateral perfusion in dogs. J Am Coll Cardiol 2000;35(2):519-26.
26. Fearon WF, Ikeno F, Bailey LR, Hiatt BL, Herity NA, Carter AJ, et al. Evaluation of high-pressure retrograde coronary venous delivery of FGF-2 protein. Catheter Cardiovasc Interv 2004;61(3):422-8.
27. von Degenfeld G, Raake P, Kupatt C, Lebherz C, Hinkel R, Gildehaus FJ, et al. Selective pressure-regulated retroinfusion of fibroblast growth factor-2 into the coronary vein enhances regional myocardial blood flow and function in pigs with chronic myocardial ischemia. J Am Coll Cardiol 2003;42(6): 1120-8.
28. Laham RJ, Rezaee M, Post M, Xu X, Sellke FW. Intrapericardial administration of basic fibroblast growth factor: myocardial and tissue distribution and comparison with intracoronary and intravenous administration. Catheter Cardiovasc Interv 2003;58(3):375-81.
29. Laham RJ, Rezaee M, Post M, Novicki D, Sellke FW, Pearlman JD, et al. Intrapericardial delivery of fibroblast growth factor-2 induces neovascularization in a porcine model of chronic myocardial ischemia. J Pharmacol Exp Ther 2000; 292(2):795-802.
30. Uchida Y, Yanagisawa-Miwa A, Nakamura F, Yamada K, Tomaru T, Kimura K, Morita T. Angiogenic therapy of acute myocardial infarction by intrapericardial injection of basic fibroblast growth factor and heparin sulfate: an experimental study. Am Heart J 1995;130(6):1182-8.
31. Lazarous DF, Shou M, Stiber JA, Dadhania DM, Thirumurti V, Hodge E, Unger EF. Pharmacodynamics of basic fibroblast growth factor: route of administration determines myocardial and systemic distribution. Cardiovasc Res 1997;36(1):78-85.
32. Zhao J, Wang Y, Wang GL, Che H, Kong XR, Liu XC. Experimental studies of intramyocardial injecting bone marrow mesenchymal stem cells combined with fibrin sealant in cells transplantation [in Chinese]. Chin J Cardiovasc Rehabil J Med 2007;16(4):321-4.
33. Zittermann SI, Issekutz AC. Endothelial growth factors VEGF and bFGF differentially enhance monocyte and neutrophil recruitment to inflammation. J Leukoc Biol 2006;80(2):247-57.
34. Anghelina M, Krishnan P, Moldovan L, Moldovan NI. Monocytes/macrophages cooperate with progenitor cells during neovascularization and tissue repair: conversion of cell columns into fibrovascular bundles. Am J Pathol 2006;168(2):529-41.
35. Blotnick S, Peoples GE, Freeman MR, Eberlein TJ, Klagsbrun M. T lymphocytes synthesize and export heparin-binding epidermal growth factor-like growth factor and basic fibroblast growth factor, mitogens for vascular cells and fibroblasts: differential production and release by CD4+ and CD8+ T cells. Proc Natl Acad Sci U S A 1994; 91(8):2890-4.
36. Martin TA, Harding KG, Jiang WG. Regulation of angiogenesis and endothelial cell motility by matrix-bound fibroblasts. Angiogenesis 1999;3(1):69-76.
37. Zhou X, Deng Y, Xie L. A study on the mechanism of bFGF promoting endothelial cells to adhere to polyurethane material [in Chinese]. Sheng Wu Yi Xue Gong Cheng Xue Za Zhi 2002;19(3):386-8.
38. Vlodavsky I, Folkman J, Sullivan R, Fridman R, Ishai-Michaeli R, Sasse J, Klagsbrun M. Endothelial cell-derived basic fibroblast growth factor: synthesis and deposition into subendothelial extracellular matrix. Proc Natl Acad Sci U S A 1987; 84(8):2292-6.
39. Pintucci G, Moscatelli D, Saponara F, Biernacki PR, Baumann FG, Bizekis C, et al. Lack of ERK activation and cell migration in FGF-2-deficient endothelial cells. FASEB J 2002; 16(6):598-600.
40. Muraoka N, Shum L, Fukumoto S, Nomura T, Ohishi M, Nonaka K. Transforming growth factor-beta3 promotes mesenchymal cell proliferation and angiogenesis mediated by the enhancement of cyclin D1, Flk-1, and CD31 gene expression during CL/Fr mouse lip fusion. Birth Defects Res A Clin Mol Teratol 2005;73(12):956-65.

41. Mountain DJ, Singh M, Menon B, Singh K. Interleukin-1 beta increases expression and activity of matrix metalloproteinase-2 in cardiac microvascular endothelial cells: role of PKCalpha/beta1 and MAPKs. Am J Physiol Cell Physiol 2007; 292(2):C867-75.
42. Yamamoto N, Kohmoto T, Roethy W, Gu A, DeRosa C, Rabbani LE, et al. Histologic evidence that basic fibroblast growth factor enhances the angiogenic effects of transmyocardial laser revascularization. Basic Res Cardiol 2000;95(1):55-63.
43. Sakakibara Y, Tambara K, Sakaguchi G, Lu F, Yamamoto M, Nishimura K, et al. Toward surgical angiogenesis using slow-released basic fibroblast growth factor. Eur J Cardiothorac Surg 2003;24(1):105-12.
44. Biswas SS, Hughes GC, Scarborough JE, Domkowski PW, Diodato L, Smith ML, et al. Intramyocardial and intracoronary basic fibroblast growth factor in porcine hibernating myocardium: a comparative study. J Thorac Cardiovasc Surg 2004;127(1):34-43.
45. Lopez JJ, Edelman ER, Stamler A, Hibberd MG, Prasad P, Caputo RP, et al. Basic fibroblast growth factor in a porcine model of chronic myocardial ischemia: a comparison of angiographic, echocardiographic and coronary flow parameters. J Pharmacol Exp Ther 1997;282(1):385-90.
46. Baffour R, Garb JL, Kaufman J, Berman J, Rhee SW, Norris MA, et al. Angiogenic therapy for the chronically ischemic lower limb in a rabbit model. J Surg Res 2000;93(2):219-29.
47. Malekan R, Reynolds C, Narula N, Kelley ST, Suzuki Y, Bridges CR. Angiogenesis in transmyocardial laser revascularization. A nonspecific response to injury. Circulation 1998; 98(19 Suppl):II62-5.
48. Chu VF, Giaid A, Kuang JQ, McGinn AN, Li CM, Pelletier MP, Chiu RC. Thoracic Surgery Directors Association Award. Angiogenesis in transmyocardial revascularization: comparison of laser versus mechanical punctures. Ann Thorac Surg 1999;68(2):301-8.
49. Lu H, Xu X, Zhang M, Cao R, Brakenhielm E, Li C, et al. Combinatorial protein therapy of angiogenic and arteriogenic factors remarkably improves collaterogenesis and cardiac function in pigs. Proc Natl Acad Sci U S A 2007;104(29):12140-5.